Optica Applicata, Vol. XI, No. 1, 1981

Producing of tolerance gaps by spatial filtering

S. V. Mikhlyaev, Yu. V. Chugui

Institute of Automation and Electrometry of Siberian Branch of the USSR Ac. of Sci., Optical Information Processing Laboratory, 630090, Novosibirsk, USSR.

I. S. Soldatenkov, T. V. Gurtova

Institute of Semiconductor Physics of Siberian Branch of the USSR Ac. of Sci., Laboratory of Basic Research in the Optoelectronics, 630090, Novosibirsk, USSR.

Method of producing the double contour images of a piece (tolerance gap) by spatial filtering is considered. The way of synthesis of splitting filter transfer function is described and the methods of its obtaining are discussed. The influence of error in producing a filter phase component on quality of tolerance gap imaging is estimated. Theoretical results are confirmed by experiments with real pieces.

1. Introduction

It is known that double contour images in the form of tolerance gaps are used effectively in solving some technical problems by optical methods. In particular, they may have the form of two contours spaced at a distance $\pm\varepsilon$ from the boundary of initial (reference) image. In the general case light amplitude in the contours may have opposite signs.

Double contour images are used, e.g. for visual control of shape and dimensions of pieces with the help of projectors [1]. In this case the tolerance gap given in a projector pattern reproduces minimal and maximal allowed dimensions of the piece, which is compared within enlarged image of the piece controlled. Another example is associated with the problem of optical image recognition. When solving this problem the use of bipolar double contour images recorded in spectral form on a holographic filter allows to realize recognition algorithms invariant with respect to contrast, photographing conditions, etc. [2].

The use of tolerance gaps faces, however, some difficulties since simple apparatus allowing their production are not available as yet. Besides, the problem of an operative production of tolerance gaps arises because of the growing demands for capacity and flexibility of optical devices. For example, projector drawings on organic glass and photographic plate do not meet these requirements, as their production as a rule is time consuming. The application of tracing paper drawings is connected with such traditional disadvantages as wearability and deformability. In case of image recognition the difficulties mentioned are aggravated by the fact that the tolerance gap must be given in bipolar form. For the formation of such fields substraction interferometers with two single contour transparencies, three-tone transparencies with subsequent filtering of constant component and phase transparencies with bipolar tolerance gap recording are used presently [2]. The facilities listed are too complicated and not universal enough. The latter means that all labour-consuming operations should be made anew, if the type of the image under recognition is to be changed.

This work was aimed to show the possibility of operative production of tolerance gaps by optical filtering with the use of reference objects (pieces or binary images). In this case tolerance gap parameters are defined by the parameters of the so-called "splitting" filter only, and configuration of the field obtained is defined by the form of reference objects. This allows to produce tolerance gaps for various objects by using the same filter.

The principle of transfer function synthesis of splitting filter is given below. The methods of its realization are discussed and experimental results from production of tolerance gaps for real pieces are presented.

2. Synthesis of splitting filters

To determine the structure of transfer function of splitting filters the problem of obtaining symmetrical tolerance gap (fig. 1b) by linear filtering of reference object (fig. 1a) should be considered. It is easy to see that the process of the tolerance gap formation in a standard coherent-optical filtering system (fig. 2) can be reduced to two operations, the first provides the contour (boundary) 1 of the object, while the second realizes its splitting

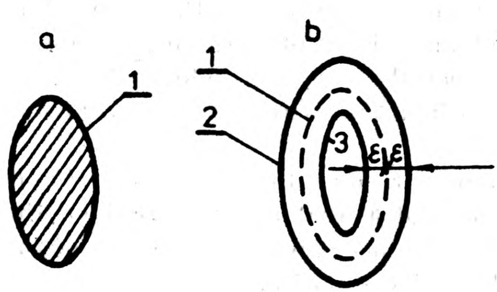

Fig .1. Schematic image of tolerance gap:
a – shadow image of the reference object, b – a tolerance gap (1 is boundary of the piece, 2 and 3 are external and internal contours of the tolerance gap)

into two components 2 and 3, corresponding to the internal and external contours of the tolerance gap (fig. 1b).

Basing on these considerations let us construct a splitting filter for one-dimensional objects (half-plane). In this case the influence of piece volume on the tolerance gap structure will be neglected.

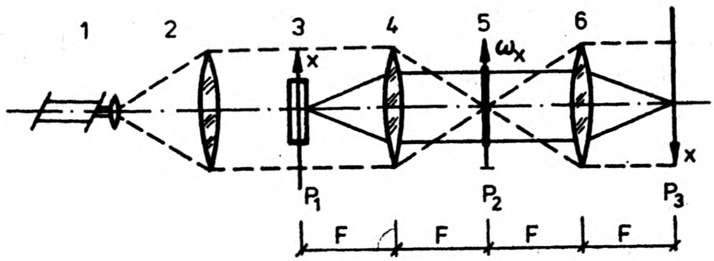

Fig. 2. Optical filtering system:
1 – laser, 2 – collimator, 3 – object, 4, 6 – objectives of direct and inverse Fourier transformations, 5 – filter

We assume that an object is placed at the input system plane P_1 (fig. 2) whose amplitude transmission $f(x)$ is described by step function (fig. 3a), i.e.

$$f(x) = Y(x). \tag{1}$$

Then by using a filter with pulse response (fig. 3b)

$$h(x) = \delta'(x-\varepsilon)-\delta'(x+\varepsilon), \tag{2}$$

where $\delta'(x)$ is the Dirac delta function derivative, we obtain at the output system plane P_3 a contour image $g(x)$ corresponding to the required tolerance gap for half-plane

$$g(x) = f(x)\otimes h(x) = \int_{-\infty}^{\infty} f(\xi)h(x-\xi)d\xi = \delta(x-\varepsilon)-\delta(x+\varepsilon). \tag{3}$$

The function $g(x)$ is given in fig. 3c.

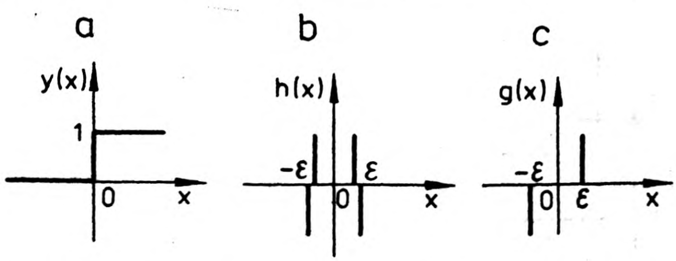

Fig. 3. Formation of tolerance gap for one-dimensional edge:
a – amplitude edge transmission $Y(x)$, b – pulse response of one-dimensional splitting filter $h(x)$, – c output distribution $g(x)$ corresponding to the tolerance gap

This filter transfer function will be as follows:

$$H(\omega_x) = \int_{-\infty}^{\infty} h(x) e^{-j\omega_x x} dx = \omega_x \sin \varepsilon\omega_x .$$

As could be expected it consists of two components: one of them provides the formation of contour, the other — its splitting.

In order to obtain the transfer function of two-dimensional splitting filter, the latter should have the following properties:

a) radial symmetry

$$\begin{aligned} h(x, y) &= h(\sqrt{x^2+y^2}), \\ H(\omega_x, \omega_y) &= H(\sqrt{\omega_x^2+\omega_y^2}), \end{aligned} \tag{4a}$$

b) "zero" reaction to constant function

$$\iint_{-\infty}^{\infty} h(x, y)\, dx dy = 0, \tag{4b}$$

c) splitting of half-plane into two contours

$$\int_{-\infty}^{x} \left\{ \int_{-\infty}^{\infty} h(x, y)\, dy \right\} dx = \frac{1}{2} [\delta(x-\varepsilon) - \delta(x+\varepsilon)]. \tag{4c}$$

It follows from the property (4a) that the filter transfer function can be found if $H(\omega_x, 0)$, i.e. one of its section, is determined. Having performed the Fourier transformation of the right- and left-hand sides of equation (4c) and using the property (4b) we can obtain

$$H(\omega_x, 0)/\omega_x = \sin \varepsilon\omega_x .$$

Then, according to (4a) the transfer function of two-dimensional splitting filter is

$$H(\omega) = \omega \sin \varepsilon\omega, \tag{5}$$

where $\omega = (\omega_x^2 + \omega_y^2)^{1/2}$.

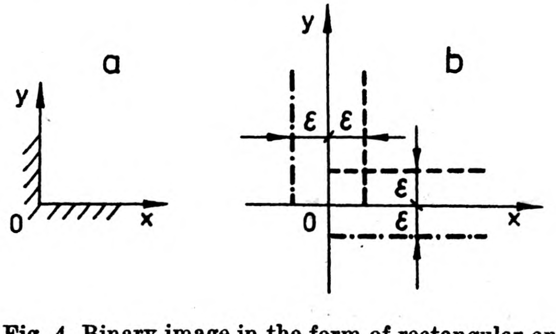

Fig. 4. Binary image in the form of rectangular angle (a), and its splitting with small ε (b)

Note that the filter (5) is obtained from the condition of half plane splitting (4c). In this connection let us consider what result may be expected if attempting to split with this filter a two-dimensional object, which has the form of an infinitely extended right angle element (fig. 4a) being described by a product of two one-dimensional step functions

$$f(x, y) = Y(x)Y(y). \tag{6}$$

The result of this object filtering may be given as

$$g(x, y) = f(x, y) \otimes h(x, y) = \frac{1}{4\pi^2} \iint\limits_{-\infty}^{\infty} F(\omega_x, \omega_y) H(\omega) e^{j(\omega_x x + \omega_y y)} d\omega_x d\omega_y, \tag{7}$$

where $F(\omega_x, \omega_y)$ is the spectrum of the object (6). Taking into account that

$$\int\limits_{-\infty}^{\infty} Y(x) e^{-j\omega_x x} dx = \pi\delta(\omega_x) + \frac{1}{j\omega_x},$$

we obtain the following expression for $g(x, y)$

$$g(x, y) = \frac{1}{2} [\delta(x-\varepsilon) - \delta(x+\varepsilon) + \delta(y-\varepsilon) - \delta(y+\varepsilon)] - g_1(x, y) \tag{8}$$

where $g_1(x, y)$ is defined as follows

$$g_1(x, y) = \frac{1}{4\pi^2} \iint\limits_{-\infty}^{\infty} \frac{\omega \sin \varepsilon\omega}{\omega_x \omega_y} e^{j(\omega_x x + \omega_y y)} d\omega_x d\omega_y. \tag{9}$$

The calculations show that when $\varepsilon \to 0$

$$g(x, y) = \frac{1}{2} [\delta(x-\varepsilon) - \delta(x+\varepsilon)] Y(y) + \frac{1}{2} [\delta(y-\varepsilon) - \delta(y+\varepsilon)] Y(x). \tag{10}$$

Function (10) is given in fig. 4b, where dotted line corresponds to its positive values and chain-dotted line — to nagative ones. It is seen from the figure that when the angle is splitted with filter (5) two contours are formed being spaced by 2ε. The line segments forming the inside contour intersect at the point $x = y = \varepsilon$, while those forming the outside contour suffer from a break when $x < 0, y < 0$.

As it may be pointed out by respective evaluations the splitting effect of an object contour takes place also for finite ε. In this case, however, the function $g(x, y)$ within the range $|x| \leqslant \varepsilon$, $|y| \leqslant \varepsilon$ may take nonzero values.

Thus the filter (5) performs ideal splitting of the half-plane boundary. When it is applied to rough boundary objects the picture of splitting becomes rather complicated in the areas of breaks. This, however, does not result in considerable distortion of tolerance gap geometry. Practically, the effects of breaking the outside contour of tolerance gap are less manifested due to finite curvature of the object boundary.

The filter proposed in [3] has analogous splitting properties but with smoother contours in splitted image. The pulse response of this filter has the form of two narrow concentric rings of radius ε, the light amplitude within their limits has the opposite sign. In this case the filter transfer function in

$$H(\omega) = \omega J_1(\varepsilon\omega), \tag{11}$$

where $J_1(\ )$ is the Bessel function of the first kind and first order. In spite of the difference between transfer function of filters (5) and (11) their structure is almost the same. They contain low frequency and high frequency components providing formation and splitting of the contour.

3. Method for producing splitting filters

Let us consider the problems of technical realization of filters with transfer functions (5) and (11). Several methods for producing such filters can be suggested. Below we shall consider the most interesting of them.

Contouring filter method

According to this method an intermediate contouring filter with transfer function ω^2 is used for synthesis of splitting filter (11).

In order to explain this method the function (11) will be written in the following form

$$H(\omega) = \frac{J_1(\varepsilon\omega)}{\omega}\,\omega^2.$$

Hence it follows that $H(\omega)$ can be presented as the product of two components, first of them corresponds to the spectrum of a hole of radius ε and the second one to transfer function of two-dimensional contouring filter.

Thus to obtain a splitting filter a spectrum of a round hole shuld be produced then modulated with a contouring unipolar filter and the resultant light distribution recorded holographically. Note that in case of nonlinear spectrum the recording can be done without contouring filter [4].

Amplitude-phase method

The above method being of holographic nature suffers from some traditional shortcomings inherently connected with this process, like light loss and geometrical distortion of the formed image [5]. Therefore, from the metrological and energetic viewpoints an amplitude-phase method of such filter synthesis is more promising although it is more labour-consuming. According to this method the splitting filter is made in the form of two components, one being of unipolar amplitude filter with transmission $H_1(\omega) = |H(\omega)|$ and the other — the binary phase filter of $H_2(\omega) = e^{j\arg H(\omega)}$ so that

$$H(\omega) = |H(\omega)|e^{j\arg H(\omega)} = H_1(\omega)H_2(\omega).$$

It should be noted that this method allows to realize the filter of both (11) and (5) types. As these filters have circular symmetry the synthesis of their amplitude components can be performed by exposing rotating light-sensitive medium through a binary area-modulated mask (fig. 5a)

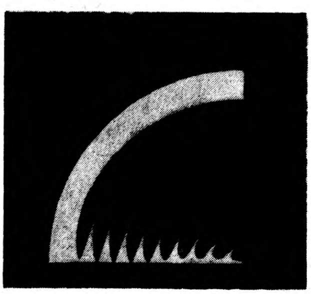

a

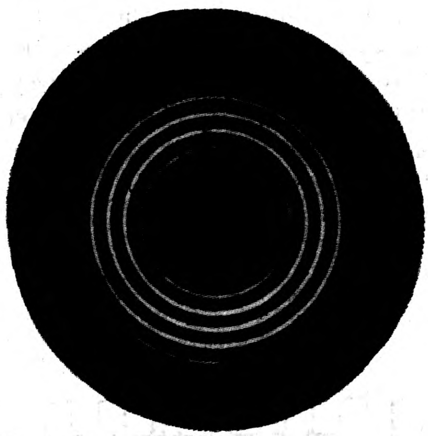

b

Fig. 5. Image of an area-modulated mask (a) used for obtaining the amplitude filter component (b)

made in polar coordinates ω, φ with the centre at the rotation axis [6, 7]. To obtain the required exposition distribution the dependence of angular size φ of the transparent mask area on the radius should have the form $\varphi = \Psi^{-1}[H_1(\omega)]$, where the function $\Psi(\varphi)$ describes nonlinearity of the recording photomaterial transmission depending on exposure. This function can be easily determined by photometering the test amplitude component, obtained with an area-modulated mask with the known law of changing φ of ω.

The phase filter component has a rather simple form

$$H_2(\omega) = \begin{cases} 1, & \text{at } H(\omega) > 0, \\ -1, & \text{at } H(\omega) < 0, \end{cases}$$

it can be realized in the form of a zone plate with a proper surface relief and provides the light wave phase shift between adjacent zones by π. The binary relief on the plate surface can be obtained by evaporating a transparent dielectrics onto a substrate [8] or ion high-frequency acattering of substrate material [9, 10], or liquid-chemical etching [11, 12].

When these methods are used the surface relief depth is obtained with an error, therefore, it is advisable to estimate the influence of this error on the tolerance gaps formed by splitting filters, thus to formulate the requirements for the accuracy of producing the phase wanted.

4. Eestimation of many featuring accuracy of phase filter component

To obtain this estimation we use the filter (5). First of all note that the realized filter is space limited by the aperture size D, i.e. $|\omega| \leqslant \omega_0 = \pi K/\varepsilon = \pi D/\lambda F$, where K is an integer of half-cycle (5) kept within the size of the filter, F is focal length of Fourier objectives, λ is light wavelength. If the phase component of the filter is constructed with the phase error β, similar for all zones of the phase plate, the frequency filter characteristic of the filter may be written as

$$\tilde{H}(\omega) = \omega \sin \varepsilon\omega e^{j\pi\beta\varphi_\varepsilon(\omega)} \operatorname{rect}(\omega/\omega_0). \tag{12}$$

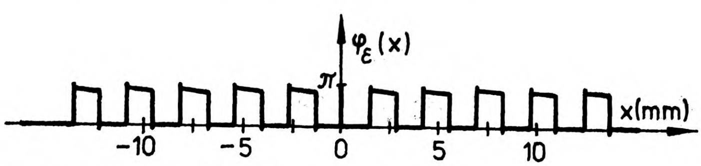

Fig. 6. Profile of phase filter component

Function $\varphi_\varepsilon(\omega)$ in (12) is a sequence of rectangular pulses of π/ε width a unit amplitude, arranged at $\omega_n = (2n-1/2)\pi/\varepsilon$, $n = 1, 2, \ldots$ points and for a space-limited filter it has the form (fig. 6)

$$\varphi_\varepsilon(\omega) = \sum_{n=1}^{N} \operatorname{rect}\left(\frac{\omega - \omega_n}{\pi/\varepsilon}\right), \tag{13}$$

where $N = \left[\frac{K}{2}\right]$, $[Z]$ is the integer of Z.

We choose the half-plane described by (1) as an input image. In the Appendix it is shown that in this case the light intensity distribution in the output image will be proportional to

$$|g(x)|^2 = \left[\frac{\varepsilon}{\pi}\frac{\sin K\pi\dfrac{x}{\varepsilon}}{x^2-\varepsilon^2}\right]^2 + \left[\frac{2\varepsilon}{\pi}\frac{1}{x^2-\varepsilon^2}\frac{\sin K\pi\dfrac{x}{2\varepsilon}}{\sin\dfrac{x}{2\varepsilon}}\right]^2 \times \sin(K+1)\frac{\pi x}{2\varepsilon}\sin(K-1)\frac{\pi x}{2\varepsilon}\sin^2\frac{\pi\beta}{2}. \quad (14)$$

From the expression (14) it is seen that the first addend describes an ideal tolerance gap and the second one describes its distortions caused by an error in manufacturing the phase filter component. When $\beta = 0$, the tolerance gap represents two sharp maxima with the amplitude $g_0 \sim (K/2\varepsilon)^2$ and width $\sim 2\varepsilon/K$, positioned at $x = \pm\varepsilon$, and a number of secondary maxima with decreasing amplitudes. Note that when apodized filters are used the level of secondary maxima can be considerably reduced. Curves of function (14) normalized by g_0 are given in fig. 7, for $x \geqslant 0$, and various

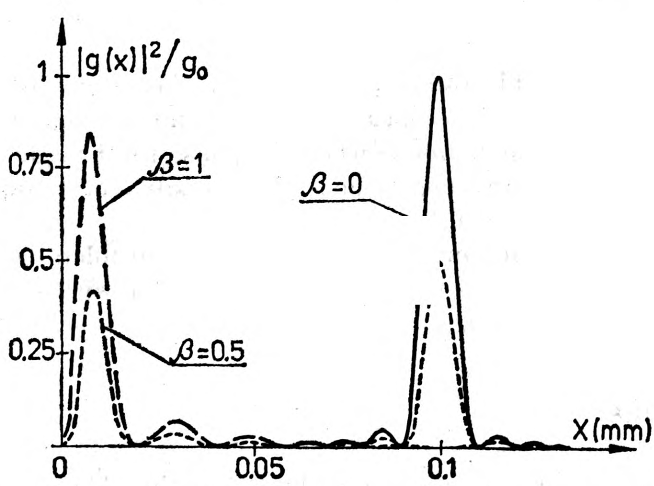

Fig. 7. Light intensity distribution over tolerance field section with phase filter error β

values of β. It may be seen that when β increases, a negligible broadening of the main maximum at $x = \varepsilon$ is obtained together with a decrease of its amplitude and increase of the amplitudes of the side maxima located at $x_n \sim 2\varepsilon n$, $n = 1, 2, \ldots$, and at $x_0 \sim 2\varepsilon/4K$, while the latter is of greater amplitude.

Let us determine now the influence of filter manufacturing error on the relative value of this maximum. It is easy to obtain from (14) that

$$I_0(\beta) = |g(x_0)|^2/g_0 = A\left(\frac{1}{2} + B\sin^2\frac{\pi\beta}{2}\right), \tag{15}$$

where

$$\begin{aligned} A &\simeq 0.41K^2/(K^2-0.56)^2, \\ B &\simeq 2.1K^2-3.41. \end{aligned} \tag{16}$$

In a similar way it is possible to determine the relative change of the main maximum level

$$I_1(\beta) = |g(\varepsilon)|^2/g_0 = \begin{cases} \cos^2\dfrac{\pi\beta}{2}, & \text{at } K \text{ even}, \\[2ex] \cos^2\dfrac{\pi\beta}{2} + \dfrac{1}{K^2}\sin^2\dfrac{\pi\beta}{2}, & \text{at } K \text{ uneven}. \end{cases} \tag{17}$$

To obtain the estimation of the maximum permissible error we demand that the side-to-the main intensity maxima ratio do not exceed α, i.e. $I_0(\beta)/I_1(\beta) \leqslant \alpha$. In this case we have from (15)–(17):

$$|\beta| \leqslant \frac{2}{\pi}\arcsin\left(\frac{\alpha - A/2}{\alpha + AB}\right)^{1/2}, \tag{18}$$

and $\alpha \geqslant A/2$.

To illustrate it with a numerical example, let $K = 10$. Then from (16) we obtain $\beta \sim 0.055$ at $\alpha = 10^{-2}$. This means that the side maximum intensity does not exceed 1% of the main one when the phase filter manufacturing error is $\sim$5%. It is interesting to note that equality of these intensities ($\alpha = 1$) is achieved at $\beta \sim 0.53$.

From the above estimations it follows that in order to obtain tolerance gaps of a good quality it is enough to manufacture phase filter with the error of β of the order of a few percents.

5. Experimental results

To support experimentally the results obtained, the filters (5), (11) with various parameters ε, K were manufactured. To make amplitude filter components the photoplates Agfa-Gefaert 8E75 were used. Taking into account nonlinearity of photomaterial transmission depending on exposure, area-modulated masks were produced with the help of a plotter with subsequent photographic decreasing up to the required size. An example of an area-modulated mask and amplitude filter component (5) obtained in this way at $K = 10$ is given in fig. 5. To decrease the level of side maxima in the resultant image apodized filters (apodizing function is $\exp[-(\omega/\omega_0)^2]$) were also made. Density curves obtained while photometering the apodized filter is given in fig. 8. Thermostatic conditions with the accuracy

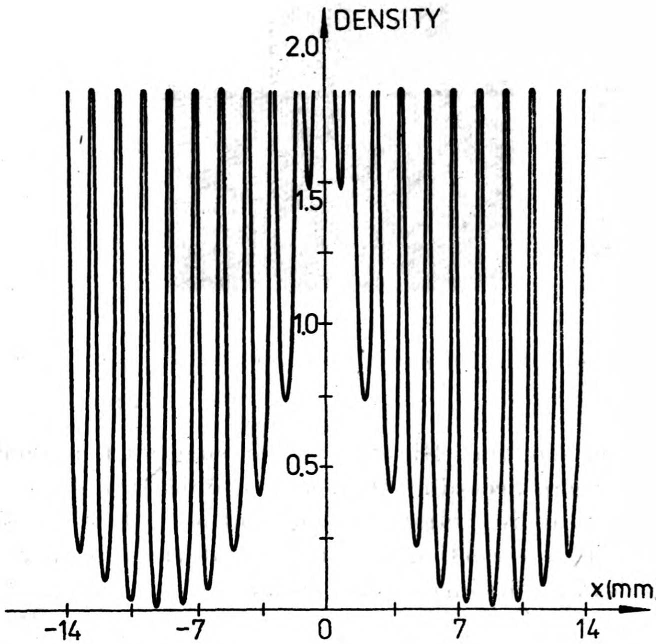

Fig. 8. Optical density distribution in the amplitude component of apodized filter

of 1 K during the production process, and invariability of chemical composition of reagents allowed to make filters with absolute transmission error equal to 5–10% within the optical density range of 0–3.

Phase filter components were made with the help of photolithography by liquid chemical etching of fused quartz. In this case the phase relief error did not exceed 1–3% which corresponds to the estimations obtained. The profile of phase filter component (5) at $K = 10$ is given in fig. 6. To estimate the quality of the formed image of tolerance gaps a test object was used in the form of a half-plane and Fourier objectives with focal length of $F = 439$ mm. Laser radiation wavelength λ was equal to 0.6328 μm. The experiments with filters (5) of $D = 28$ mm and the number of zones $K = 10$ and 20 tolerance gaps were obtained with ε equal to 0.1 and 0.2 mm, respectively. This is in a good agreement with theoretical value of ε determined from the formula $\varepsilon = K\lambda F/D$ and equal to 0.099 mm ($K = 10$). Phase components made with different error ($\leqslant 3\%$) did not display any considerable differences in the resultant images as it should be expected.

The figures 9a, b represent the photographs of tolerance gaps formed by splitting filters (5) at $K = 10$ and $K = 20$, for real objects of complicated form. It should be noted that the quality of the images is much better than that obtained in [3] with a holographic filter.

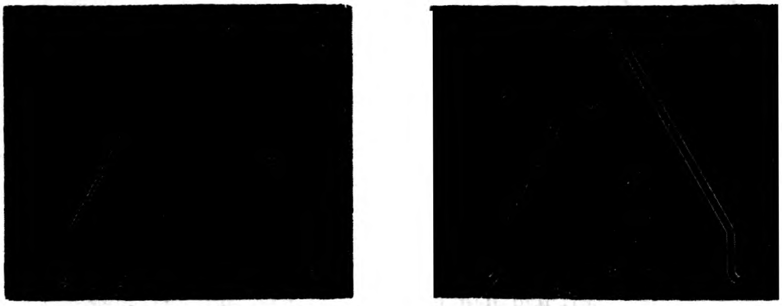

a b

Fig. 9. Tolerance fields for real objects of complicated form at $K = 10$ (a) and $K = 20$ (b)

Experimental results confirm the efficiency of the suggested method for production of tolerance gap according to reference objects and show the possibility of its practical realization in coherent-optical systems. This method can be used in construction of automatic devices for shape and size controlling articles and for image recognition.

Appendix

Let us calculate the light intensity distribution $|g(x)|^2$ in half-plane image (1) in case of its filtering with splitting filter (12) with the phase error β.

Since the result of filtering (tolerance gap) is defined by the expression

$$g(x, y) = \frac{1}{4\pi^2} \iint\limits_{-\infty}^{\infty} F(\omega_x, \omega_y)\, \tilde{H}(\omega)\, e^{j(\omega_x x + \omega_y y)} d\omega_x d\omega_y, \tag{1A}$$

then using the known result

$$F(\omega_x, \omega_y) = 2\pi\delta(\omega_y)\left[\pi\delta(\omega_x) + \frac{1}{j\omega_x}\right],$$

and taking account of (12) we reduce (1A) to the form

$$g(x) = \frac{1}{2\pi j} \int\limits_{-\infty}^{\infty} \sin \omega\varepsilon_x e^{j\beta\pi\varphi_\varepsilon(\omega_x)} e^{j\omega_x x} d\omega_x = \frac{1}{2} [\delta(x-\varepsilon) - \delta(x+\varepsilon)] \otimes g_1(x), \tag{2A}$$

where

$$g_1(x) = \frac{1}{2\pi} \int\limits_{-\infty}^{\infty} e^{j\beta\pi\varphi_\varepsilon(\omega_x)} e^{j\omega_x x} d\omega_x.$$

Using (13) we can obtain

$$g_1(x) = 2\frac{\sin\frac{\pi x}{2\varepsilon}}{\pi x}\left\{\sum_{n=1}^{N}\left[e^{j\beta\pi}\cos\frac{\pi x}{\varepsilon}\left(2n-\frac{1}{2}\right)+\cos\frac{\pi x}{\varepsilon}\left(2n-\frac{3}{2}\right)\right.\right.$$
$$\left.\left.+\cos\frac{\pi x}{\varepsilon}\left(2N+\frac{1}{2}\right)\right\}. \tag{3A}$$

Note that if the function (13) contains an even number of half-cycles kept K in the size of the filter, the latter added in (3A) is absent.

Taking into consideration that

$$\sum_{n=1}^{N}\cos(na) = \cos\frac{N+1}{2}a\sin\frac{N}{2}a/\sin\frac{a}{2},$$

$$\sum_{n=1}^{N}\sin(na) = \sin\frac{N+1}{2}a\sin\frac{N}{2}a/\sin\frac{a}{2},$$

and reducing (3A) to the following form

$$g_1(x) = \frac{1}{\pi x}\frac{\sin N\pi\frac{x}{\varepsilon}}{\cos\frac{\pi x}{2\varepsilon}}\left[e^{j\beta\pi}\cos\left(N+\frac{1}{2}\right)\frac{\pi x}{\varepsilon}+\cos\left(N-\frac{1}{2}\frac{\pi x}{\varepsilon}\right]\right., \quad \text{for even } K$$

$$g_1(x) = \frac{1}{\pi x}\frac{\sin N\pi\frac{x}{\varepsilon}}{\cos\frac{\pi x}{2\varepsilon}}\left[e^{j\beta\pi}\cos\left(N+\frac{1}{2}\right)\frac{\pi x}{\varepsilon}+\cos\left(N-\frac{1}{2}\right)\frac{\pi x}{\varepsilon}\right]$$
$$+\frac{2}{\pi x}\sin\frac{\pi x}{2\varepsilon}\cos\left(2N+\frac{1}{2}\right)\frac{\pi x}{\varepsilon}, \quad \text{for odd K.} \tag{4A}$$

:Accordingly from (2A) the following expression for a filtered image can be obtained

$$|g(x)|^2 = \left[\frac{\varepsilon}{\pi}\frac{\sin\frac{K\pi x}{\varepsilon}}{x^2-\pi^2}\right]^2+\left[\frac{2\varepsilon}{\pi(x^2-\varepsilon^2)}\frac{\sin\frac{K\pi x}{2\varepsilon}}{\sin\frac{\pi x}{2\varepsilon}}\right]^2$$
$$\times\sin(K+1)\frac{\pi x}{2\varepsilon}\sin(K-1)\frac{\pi x}{2\varepsilon}\sin^2\frac{\pi\beta}{2}. \tag{5A}$$

References

[1] IVANOV A. G., *Izmeritelnie pribory v mashinostroenii*, Mashinostroenie, Moskva 1964.

[2] KOZLOV O. A., et al., Avtometriya **6** (1976), 36.

[3] MIKHLYAEV S. V., CHUGUI Yu. V., Avtometriya **1** (1979), 24.

[4] BEKKER A. M., et al., [In:] *Opticheskaya obrabotka informatsii*, ed. by GUREVITCH S. B., Nauka, Leningrad 1978, p. 50.

[5] VANDER LUGT A., Appl. Opt. **5** (1966), 1766.
[5] KRIVENKOV B. E., CHUGUI Yu. V., Avtometriya **1** (1979), 33.
[6] STROKE G. W., et al., Optik **41** (1974), 319.
[7] FIRESTER A. H., et al., Opt. Commun. **8** (1973), 160.
[8] SMIT G., Proc. IEEE **10** (1975), 78.
[9] BOBROV S. T., et al., [In:] *Holografitcheskie izmeritelnie sistemy*, ed. by A. G. KOZATCHOK, Novosibirsk 1978, p. 123.
[10] BURCKHARDT C. B., Appl. Opt. **9** (1970), 695.
[11] LEVIN V. Yu., et al., Opt. Mekh. Prom. **45**, 3 (1978), 43.

Received May 6, 1980

Формирование полей допусков посредством пространственной фильтрации

Рассмотрен способ формирования двойного контурного изображения изделия (поля допусков) посредством пространственной фильтрации. Описывается метод синтеза передаточной функции расщепляющего фильтра, обсуждаются методики его получения. Оценивается влияние погрешности изготовления фазовой компоненты фильтра на качество изображения поля допусков. Теоретические результаты подтверждаются экспериментами с реальными изделиями.